

Simulation of stirred flow reactor

*M. VAJDA, ^bJ. ILAVSKÝ, and ^cJ. PISOŇ

^aDepartment of Chemical Engineering, Slovak Technical University,
812 37 Bratislava

^bDepartment of Organic Technology, Slovak Technical University,
812 37 Bratislava

^cHarmanec Paper Mill,
976 03 Harmanec

Received 28 July 1980

Accepted for publication 3 August 1981

Three combined models were proposed for a stirred flow reactor. The suitability of these models was appreciated by means of the measured E functions. The parameters of model were determined by the simplex method. Owing to good agreement with experiments and mathematical simplicity, the model comprising two differently large and perfectly stirred regions connected in series and one deadwater region was selected as the most convenient of the investigated three models.

Для проточного перемешиваемого реактора были предложены три комбинированные модели. На основании измеренных E функций была определена адекватность предложенных моделей. Параметры модели определялись методом симплексов. На основании хорошего согласия с экспериментом и ради математической простоты была избрана модель, состоящая из двух неодинаково больших идеально перемешиваемых пространств в серии и из недейственного пространства.

Many authors were concerned with simulation of a real stirred flow reactor (SFR). In this way, the papers by *van de Vusse* [1], *Oyama* [2], *Cholette* [3] as well as the papers by other authors [4—8] are known.

We started from the ideas of these authors in our attempt to devise a model of stirred flow reactor. The models advanced by us comprise a region of perfect stirring and a deadwater region as well as a short stream and recirculating flow.

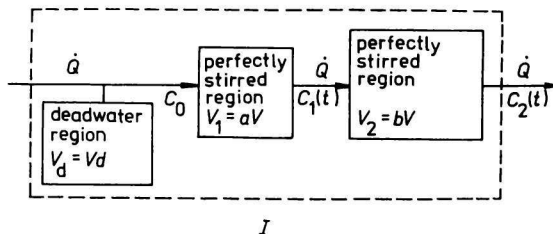


Fig. 1. Model I.

The first (two-parameter) model comprises two differently large regions of perfect stirring (aV and bV) and a deadwater region (dV) (Fig. 1).

For the distribution function of the residence time we may write

$$E(\Theta) = \frac{1}{a-b} \left[e^{-\frac{\Theta}{a}} - e^{-\frac{\Theta}{b}} \right] \quad (1)$$

where

$$\Theta = \frac{\dot{Q}t}{V} \quad (2)$$

This expression is to be obtained by solving the system of the following two differential equations

$$aV \frac{dC_1}{dt} = \dot{Q}(C_0 - C_1) \quad (3)$$

$$bV \frac{dC_2}{dt} = \dot{Q}(C_1 - C_2)$$

where

$$C_0 = C^0 \delta(t) \quad (4)$$

For calculating the mean residence time and mean age we may derive the following equations

$$\bar{\Theta}_E = \frac{1}{a-b} \int_0^\infty \Theta \left[e^{-\frac{\Theta}{a}} - e^{-\frac{\Theta}{b}} \right] d\Theta = a + b \quad (5)$$

$$\bar{\Theta}_1 = \frac{1}{a-b} \int_0^\infty \Theta \left[ae^{-\frac{\Theta}{a}} - be^{-\frac{\Theta}{b}} \right] d\Theta = a^2 + b^2 + ab \quad (6)$$

The dispersion is to be calculated by solving the equation

$$\sigma_E^2 = \frac{1}{a-b} \int_0^\infty \left[\Theta^2 - 2\Theta\bar{\Theta}_E + \bar{\Theta}_E^2 \right] \left[e^{-\frac{\Theta}{a}} - e^{-\frac{\Theta}{b}} \right] d\Theta = a^2 + b^2 \quad (7)$$

It is evident that

$$a + b \leq 1 \quad (8)$$

The equality of relation (8) is fulfilled if $d=0$.

The second (three-parameter) model differs from the first one in that the first region of perfect stirring is bypassed by a short stream (Fig. 2).

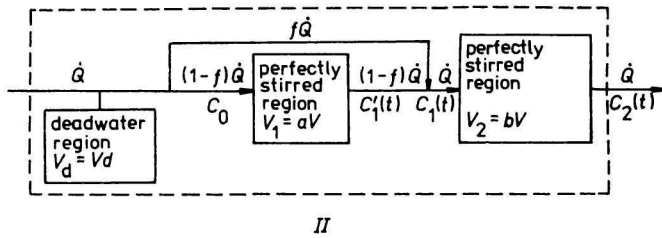


Fig. 2. Model II.

The distribution function of the residence time may be obtained, for instance, by solving the convolution integral

$$E(\Theta) = \int_0^{\Theta} E_1(s) E_2(\Theta - s) ds \quad (9)$$

where

$$E_1(s) = \frac{(1-f)^2}{a} e^{-\frac{1-f}{a}s} + f\delta(s) \quad (10)$$

is the Laplace transform of the distribution of the residence time for the first region of perfect stirring with bypass flow and it holds

$$E_2(\Theta - s) = \frac{1}{b} e^{-\frac{\Theta-s}{b}} \quad (11)$$

For the distribution function of the residence time of the second model we obtain

$$E(\Theta) = \left[\frac{f}{b} - \frac{(1-f)^2}{a - (1-f)b} \right] e^{-\frac{\Theta}{b}} + \frac{(1-f)^2}{a - (1-f)b} e^{-\frac{1-f}{a}\Theta} \quad (12)$$

because it holds [9, 10]

$$\int_0^{\Theta} \delta(s) e^{\frac{s}{b}} ds = 1 \quad (13)$$

The following expressions may be derived for calculating the mean residence time and mean age

$$\bar{\Theta}_E = \frac{a^2 + fab - (1-f)b^2}{a - (1-f)b} \quad (14)$$

$$\bar{\Theta}_1 = \frac{ab^2f(1-f) - [1 + 2f(1-f)]b^3 + a^3}{[a - (1-f)b](1-f)} \quad (15)$$

The dispersion is to be calculated from the following equation

$$\sigma_E^2 = 2b^3 K_1 + 2b^2 \bar{\Theta}_E K_1 + b \bar{\Theta}_E^2 K_1 + 2 \left(\frac{a}{1-f} \right)^3 K_2 + 2 \left(\frac{a}{1-f} \right)^2 \bar{\Theta}_E K_2 + \frac{a}{1-f} \bar{\Theta}_E^2 K_2 \quad (16)$$

where

$$K_1 = \frac{f}{b} - \frac{(1-f)^2}{a - (1-f)b} \quad (16a)$$

and

$$K_2 = \frac{(1-f)^2}{a - (1-f)b} \quad (16b)$$

The third (four-parameter) model differs from the first one by including further region of perfect stirring (Fig. 3) into recirculating flow.

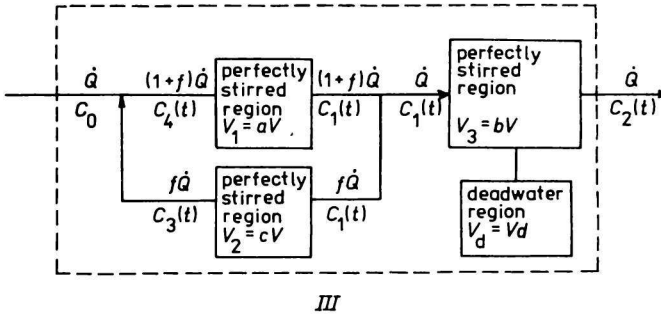


Fig. 3. Model III.

From material balance, we obtain for total transfer function of model this expression

$$E(s) = \frac{C_2(s)}{C_0(s)} = \frac{E_2(s) E_1(s)}{(1+f) - fE_1(s) E_2(s)} \quad (17)$$

while

$$C_1(s) = E_1(s) C_4(s) \quad (17a)$$

$$C_2(s) = E_3(s) C_1(s) \quad (17b)$$

$$C_3(s) = E_2(s) C_1(s) \quad (17c)$$

and

$$E_1(s) = \frac{1}{\frac{a}{1+f} s + 1} \quad (18a)$$

$$E_2(s) = \frac{1}{\frac{bs}{f} + 1} \quad (18b)$$

$$E_3(s) = \frac{1}{cs + 1} \quad (18c)$$

By inserting expressions (18a—c) into eqn (17), rearranging, and using reverse transformation, we obtain the E function

$$E(\Theta) = B_3[Ae^{-B_1\Theta} + Be^{-B_2\Theta} + De^{-B_3\Theta}] \quad (19)$$

where

$$A = \frac{1 - A_2B_1}{(B_2 - B_1)(B_3 - B_1)} \quad (19a)$$

$$B = \frac{1 - A_2B_2}{(B_1 - B_2)(B_3 - B_2)} \quad (19b)$$

$$D = \frac{1 - A_2B_3}{(B_1 - B_3)(B_2 - B_3)} \quad (19c)$$

and

$$A_1 = \frac{a}{1 + f} \quad (20a)$$

$$A_2 = \frac{b}{f} \quad (20b)$$

$$B_1 = \frac{(1 + f)(A_1 + A_2) + \sqrt{DD}}{2(1 + f) A_1 A_2} \quad (21a)$$

$$B_2 = \frac{(1 + f)(A_1 + A_2) - \sqrt{DD}}{2(1 + f) A_1 A_2} \quad (21b)$$

$$DD = [(1 + f)(A_1 + A_2)]^2 - 4(1 + f) A_1 A_2 \quad (21c)$$

$$B_3 = \frac{1}{c} \quad (21d)$$

It may be proved that the discriminant DD in eqns (21a, b) assumes only positive values for $f > 0$.

The following expressions may be derived for calculating the mean residence time and dispersion

$$\bar{\Theta}_E = B_3 \left(\frac{A}{B_1^2} + \frac{B}{B_2^2} + \frac{D}{B_3^2} \right) \quad (22)$$

$$\sigma_E^2 = B_3 \left[2A \left(\frac{1}{B_1^3} + \frac{\bar{\Theta}_E}{B_1^2} + \frac{\bar{\Theta}_E^2}{2B_1} \right) + 2B \left(\frac{1}{B_2^3} + \frac{\bar{\Theta}_E}{B_2^2} + \frac{\bar{\Theta}_E^2}{2B_2} \right) + 2D \left(\frac{1}{B_3^3} + \frac{\bar{\Theta}_E}{B_3^2} + \frac{\bar{\Theta}_E^2}{2B_3} \right) \right] \quad (23)$$

Experimental

The experimental device is schematically outlined in Fig. 4. It consisted of a stirred flow reactor SFR 1 in which distilled water flowed from stock tanks 5 (simultaneously from both). The flow was controlled by needle valves 7 and measured with rotameters 8. Both flows were mixed immediately before entrance into SFR. In this short common section of 2 cm length there was a hole 9 where the tracer was injected by means of a syringe. The response was measured at the exit from SFR. A conductivity sensor was placed in a glass tube 10 with a side hole — about 4 cm over SFR. The conductivity sensor consisted of two platinum wires of 1 mm diameter and 2 cm length protruding from a teflon body. The conductance was measured with a conductoscope (made according to the scheme put forward in [11]) connected with a recorded EZ-4. The temperature in reactor was measured with a thermometer 11 graduated in 0.1°C.

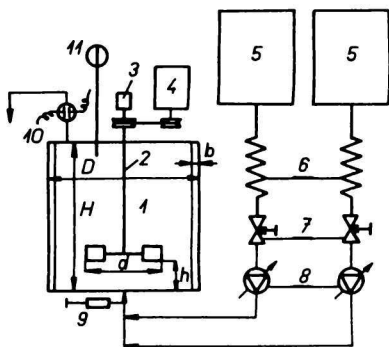


Fig. 4. Experimental device.

1. Reactor ($D = 0.137$ m, $H = 0.189$ m, $h = 0.034$ m, $d = 0.035$ m, $b = 0.014$ m); 2. shaft; 3. tachodynamo; 4. electromotor ROME; 5. stock tanks; 6. exchangers of heat; 7. needle control valves; 8. rotameters; 9. inlet of tracer; 10. conductivity sensor; 11. thermometer.

The proper SFR consisted of a glass cylinder the bases of which were made of stainless steel. The inlet was in the bottom base whereas the outlet was in the upper base. The axis of the stirrer was driven by an electromotor ROME with changeable revolutions. The stirrer was attached at the end of the axis. Three types of stirrers were used:

1. turbine stirrer 1 with straight perpendicular vanes and dividing wheel ON 69 10 21 (Fig. 5);
2. turbine stirrer 2 with straight oblique vanes ON 69 10 20 (Fig. 6);
3. turbine stirrer 3 with wing vanes ON 09 10 24 (Fig. 7).

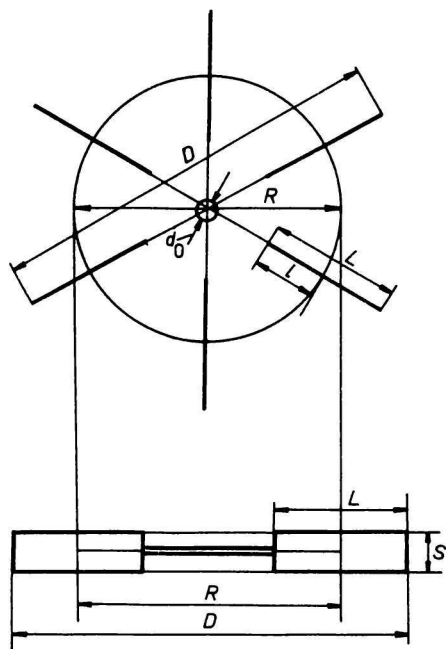


Fig. 5. Turbine 1.

$D=0.046$ m, $R=0.0307$ m, $L=0.0154$ m, $S=$
 $=0.0075$ m, $l=0.0077$ m, $d_0=0.0032$ m.

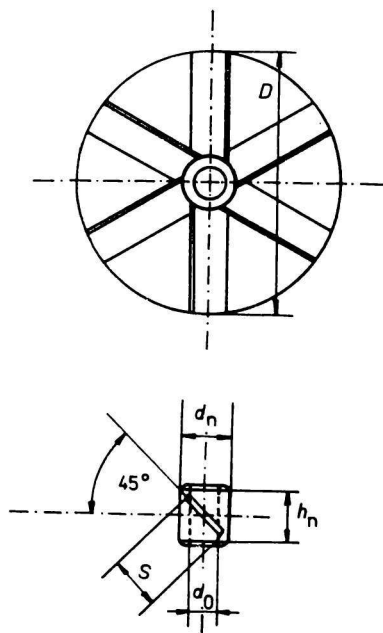


Fig. 6. Turbine 2.

$D=0.0343$ m, $d_n=0.0069$ m, $d_0=0.0032$ m,
 $h_n=0.0069$ m, $S=0.0069$ m.

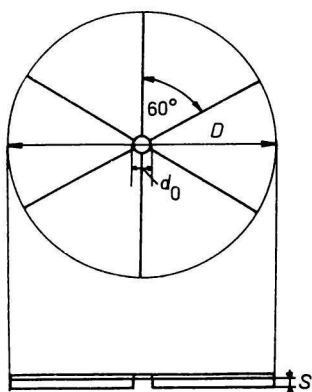


Fig. 7. Turbine 3.

$D = 0.046$ m, $S = 0.002$ m, $d_0 = 0.0032$ m.

Four exchangeable baffles were placed inside the reactor. The characteristics of liquid flow were ascertained from the distribution of the residence time in the reactor. The distribution function of the residence time $E(\Theta)$ was determined by the method of stimulus and response. The stimulus — simulation of the $\delta(\Theta)$ function — was accomplished by injecting about 2 cm^3 of almost saturated solution of KCl in a very short time moment. The response was investigated by measuring the conductivity at the outlet from the reactor. As the earthing was problematic, the measurements were carried out in the regime of the so-called floating potential. Before each measurement, the zero position of the recorder was fixed (with respect to distilled water). The measurement of response was finished when the recorder stylus returned into zero position. During experiment the temperature was held constant accurate to $\pm 0.1^\circ\text{C}$. The linear dependence of conductivity on concentration of the tracer was verified by comparing the colorimetric method with the conductivity method.

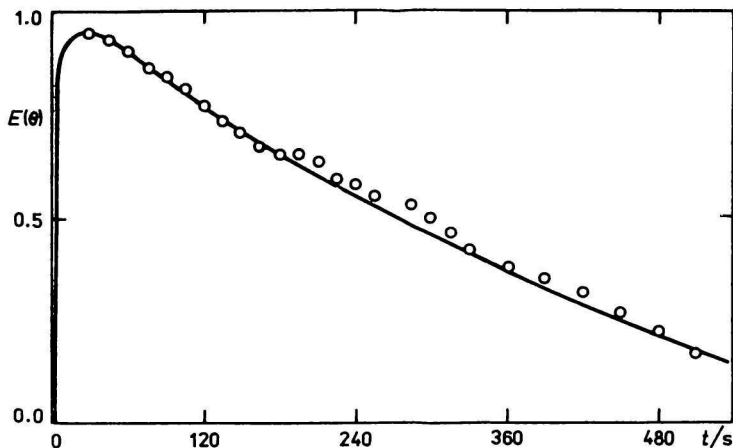


Fig. 8. Comparison of conductivity record with colorimetric determination of the tracer.
 — Conductivity record; \circ colorimetric determination.

A solution of $K_2Cr_2O_7$ was used as tracer. Simultaneously with conductivity measurement the samples for colorimetric determination were taken in 15 s intervals. The values of absorbance obtained by means of a spectral photocolormeter Spekol were multiplied by the constant k and plotted in the conductivity record (Fig. 8). The agreement of both methods was good within the whole investigated concentration range.

Results and discussion

As for the parameters of the proposed mathematical models, those values for which the minimization function assumes the minimum are regarded as values sought for (criterion of accordance). The following expression was assumed to be the minimization function

$$U(a, b, c, f) = \sum_{i=1}^n [E_{ci}(\Theta) - E_{ci}(\Theta)]^2 \quad (24)$$

where n is the number of selected points from the continuous conductivity record.

The seeking for the parameters was carried out by the simplex method. The values determined from the maximum of the E curve [12] (or from the point of inflection) were used for fixing the starting values of the parameters. It holds for the value Θ in the maximum of the curve corresponding to model I

$$\Theta_{\max} = \frac{(\sqrt{ab})^2}{a-b} \ln \frac{a}{b} \quad (25)$$

and in the point of inflection

$$\Theta_{\inf} = \frac{ab \ln \left(\frac{a}{b}\right)^2}{a-b} \quad (26)$$

The value of Θ_{\max} is to be determined more precisely on the basis of experiments. Then it is possible to determine the values of the parameters a and b from the equality

$$a + b + d = 1 \quad (27)$$

and eqn (25) by using iteration and the relationship

$$b_{i+1} = 1 - d - \frac{\Theta_{\max}}{b_i} \frac{1 - d - 2b_i}{\ln \left(\frac{1 - b_i - d}{b_i}\right)} \quad (28)$$

The value of the parameter d is to be determined from the value of $\bar{\Theta}_E$ found experimentally for the time (Θ) interval 0—3 and spatial time $\tau = V\dot{Q}^{-1}$.

The tightness of the experimental curve with respect to the calculated values is evident in Fig. 9. The parameter f characterizing the short stream in model *II* was negligible under all conditions owing to which model *II* was reduced to model *I*. Besides, the value of f characterizing the magnitude of recirculating flow and the value of c (portion of the magnitude of the perfectly stirred region in the recirculating flow) of model *III* were insignificant.

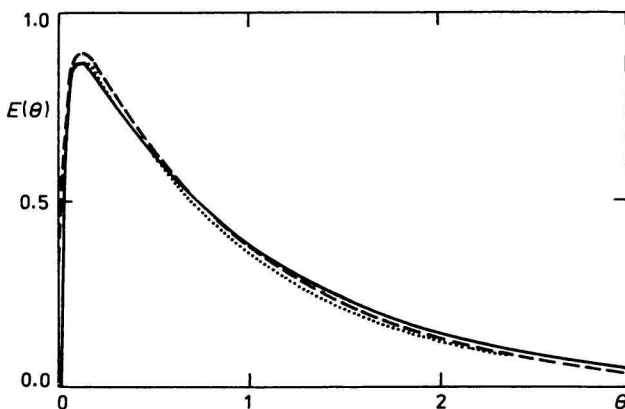


Fig. 9. Comparison of experimental values with calculated values for models *I*, *II*, and *III*.
— Conductivity record; - - - models *I* and *II*; . . . model *III*.

The tightness of the experimental curve with respect to the calculated curve with optimum coefficients was appreciated on the basis of the value of the regression coefficient calculated from the equation

$$R_c = \frac{\sum_{i=1}^n (E_{ei} E_{ci}) - \sum_{i=1}^n E_{ei} \sum_{i=1}^n E_{ci}}{\sqrt{\left[n \sum_{i=1}^n E_{ei}^2 - \left(\sum_{i=1}^n E_{ei} \right)^2 \right] \left[n \sum_{i=1}^n E_{ci}^2 - \left(\sum_{i=1}^n E_{ci} \right)^2 \right]}} \quad (29)$$

The values of the parameters for model *I* and model *III* are given in Tables 1—3. The last column of table contains the regression coefficient calculated on condition that SFR is regarded as a perfect stirrer.

From the results obtained it follows that our approach based on the simple idea of connection of differently large perfect stirrers is conformable to reality under all investigated conditions for the distribution of the residence time in SFR. The

Table 1
Turbine 1

$\frac{\dot{Q} \cdot 10^5}{\text{m}^3 \text{s}^{-1}}$	ω/s^{-1}	Model I			Model III					IM R_{CIM}
		<i>a</i>	<i>b</i>	R_c	<i>a</i>	<i>b</i>	<i>c</i>	<i>f</i>	R_c	
1.0	4.17	0.108	0.830	0.9857	0.732	0.001	0.115	0.001	0.9846	0.8684
	8.33	0.063	0.937	0.9896	0.808	0.066	0.066	0.061	0.9855	0.9528
	12.5	0.059	0.941	0.9892	0.817	0.060	0.064	0.055	0.9876	0.9107
	16.7	0.063	0.937	0.9876	0.828	0.056	0.063	0.052	0.9845	0.8864
	20.8	0.041	0.959	0.9953	0.905	0.027	0.041	0.027	0.9940	0.9397
	25.0	0.049	0.951	0.9922	0.894	0.029	0.050	0.027	0.9909	0.9178
	33.3	0.037	0.963	0.9959	0.961	0.001	0.036	0.001	0.9965	0.9470
1.33	4.17	0.255	0.745	0.9751	0.896	0.001	0.099	0.001	0.9740	0.8243
	8.33	0.155	0.845	0.9813	0.854	0.034	0.081	0.031	0.9898	0.8610
	12.5	0.135	0.865	0.9820	0.938	0.001	0.060	0.001	0.9919	0.8876
	16.7	0.108	0.892	0.9852	0.905	0.019	0.059	0.018	0.9914	0.8956
	20.8	0.122	0.878	0.9824	0.905	0.001	0.063	0.001	0.9908	0.8831
	25.0	0.102	0.897	0.9863	0.874	0.037	0.055	0.035	0.9925	0.9108
	33.3	0.105	0.895	0.9844	0.883	0.032	0.055	0.031	0.9923	0.9084
1.67	4.17	0.148	0.663	0.9876	0.636	0.002	0.147	0.001	0.9870	0.8628
	8.33	0.105	0.895	0.9869	0.810	0.001	0.106	0.001	0.9861	0.8945
	12.5	0.076	0.924	0.9936	0.841	0.044	0.075	0.041	0.9914	0.8935
	16.7	0.074	0.926	0.9920	0.918	0.005	0.072	0.005	0.9911	0.8832
	20.8	0.072	0.928	0.9924	0.935	0.001	0.063	0.001	0.9914	0.8921
	25.0	0.055	0.945	0.9969	0.861	0.041	0.059	0.039	0.9950	0.9302
	33.3	0.050	0.950	0.9974	0.893	0.030	0.048	0.029	0.9954	0.9391

Table 1 (Continued)

$\frac{\dot{Q} \cdot 10^5}{\text{m}^3 \text{ s}^{-1}}$	ω/s^{-1}	Model I			Model III					IM R_{CIM}
		<i>a</i>	<i>b</i>	R_c	<i>a</i>	<i>b</i>	<i>c</i>	<i>f</i>	R_c	
2.0	4.17	0.196	0.794	0.9857	0.869	0.001	0.123	0.001	0.9708	0.8233
	8.33	0.115	0.885	0.9877	0.871	0.002	0.112	0.002	0.9881	0.8305
	12.5	0.060	0.939	0.9893	0.933	0.007	0.060	0.005	0.9914	0.9130
	16.7	0.072	0.928	0.9887	0.924	0.005	0.070	0.003	0.9908	0.8843
	20.8	0.058	0.942	0.9921	0.920	0.013	0.060	0.001	0.9927	0.9202
	25.0	0.071	0.929	0.9934	0.913	0.015	0.070	0.002	0.9917	0.9256
	33.3	0.054	0.946	0.9897	0.916	0.031	0.050	0.001	0.9920	0.9327

Table 2

Turbine 2

$\frac{\dot{Q} \cdot 10^5}{\text{m}^3 \text{ s}^{-1}}$	ω/s^{-1}	Model I			Model III					IM R_{CIM}
		<i>a</i>	<i>b</i>	R_c	<i>a</i>	<i>b</i>	<i>c</i>	<i>f</i>	R_c	
1.0	4.17	0.075	0.925	0.9853	0.921	0.001	0.073	0.001	0.9852	0.8766
	8.33	0.035	0.965	0.9949	0.916	0.027	0.031	0.026	0.9925	0.9523
	12.5	0.036	0.946	0.9968	0.963	0.001	0.034	0.002	0.9966	0.9563
	16.7	0.034	0.966	0.9984	0.922	0.023	0.031	0.023	0.9963	0.9632
	20.8	0.037	0.963	0.9972	0.962	0.001	0.036	0.001	0.9971	0.9533
	25.0	0.038	0.962	0.9963	0.934	0.015	0.037	0.015	0.9954	0.9479
	33.3	0.039	0.961	0.9976	0.902	0.031	0.036	0.031	0.9944	0.9496

Table 2 (Continued)

$\frac{\dot{Q} \cdot 10^5}{\text{m}^3 \text{ s}^{-1}}$	ω/s^{-1}	Model I			Model III					IM R_{CIM}
		<i>a</i>	<i>b</i>	R_c	<i>a</i>	<i>b</i>	<i>c</i>	<i>f</i>	R_c	
1.67	4.17	0.085	0.915	0.9882	0.885	0.001	0.085	0.001	0.9886	0.9239
	8.33	0.086	0.914	0.9901	0.885	0.001	0.081	0.001	0.9903	0.8757
	12.5	0.046	0.954	0.9988	0.959	0.001	0.038	0.001	0.9973	0.9527
	16.7	0.056	0.944	0.9965	0.946	0.001	0.052	0.001	0.9961	0.9297
	20.8	0.053	0.947	0.9970	0.894	0.026	0.054	0.025	0.9958	0.9337
	25.0	0.056	0.944	0.9970	0.938	0.001	0.056	0.001	0.9970	0.9299
	33.3	0.040	0.960	0.9992	0.890	0.036	0.038	0.035	0.9965	0.9596

Table 3
Turbine 3

$\frac{\dot{Q} \cdot 10^5}{\text{m}^3 \text{ s}^{-1}}$	ω/s^{-1}	Model I			Model III					IM R_{CIM}
		<i>a</i>	<i>b</i>	R_c	<i>a</i>	<i>b</i>	<i>c</i>	<i>f</i>	R_c	
1.0	4.17	0.197	0.766	0.9679	0.732	0.036	0.205	0.027	0.9663	0.7383
	8.33	0.098	0.902	0.9804	0.820	0.018	0.106	0.016	0.9806	0.8727
	12.5	0.064	0.936	0.9864	0.891	0.014	0.089	0.022	0.9875	0.9330
	16.7	0.046	0.954	0.9953	0.923	0.015	0.052	0.012	0.9978	0.9284
	20.8	0.060	0.940	0.9896	0.934	0.010	0.050	0.007	0.9908	0.8957
	25.0	0.067	0.933	0.9857	0.916	0.013	0.066	0.011	0.9897	0.8741
	33.3	0.046	0.954	0.9945	0.945	0.010	0.040	0.002	0.9951	0.9304

influence of different conditions on magnitude of the perfectly stirred regions is most conspicuous in case of model *I*. The magnitude of the first perfectly stirred region is most significantly affected by the type of stirrer. For turbine stirrers *1* and *3* with dividing wheel with which the formation of two circulating loops in SFR manifests itself more, the values of *a* are greater than those for stirrer *2*.

The portion of the magnitude of the first perfectly stirred region *a* decreases with increasing frequency of revolutions of the stirrer for all flows while it slightly increases with flow at equal revolutions.

The values of the regression coefficient increase with revolutions. It is due to the fact that a) the tracer was not uniformly stirred at lower revolutions at the beginning of experiments owing to which the measured response was not smoothed, b) the curves of response exhibited a certain temporal shift between the time moment of stimulus and the beginning of response.

Three models of stirred flow reactor were proposed and experimentally tested. Among them model *I* appeared to be the best. The *E* curves calculated on the basis of this model are in good agreement with experimental results. It is also notable that this model is to be represented by simple mathematical functions.

Symbols

<i>a</i>	parameter of model equal to a part of total volume of SFR
<i>b</i>	parameter of model equal to a part of total volume of SFR
<i>c</i>	parameter of model equal to a part of total volume of SFR
<i>d</i>	parameter of model equal to a part of total volume of SFR
<i>f</i>	parameter of model, ratio of the flow of bypass flow to total flow
<i>C</i>	tracer concentration
<i>C</i> ⁰	characteristic concentration
<i>E</i> (Θ)	residence time distribution function
<i>R</i> _c	regression coefficient
\dot{Q}	volume flow
<i>s</i>	Laplace variable
<i>t</i>	time
<i>V</i>	volume of reactor
Θ	dimensionless time
τ	spatial time
$\delta(\Theta)$	Dirac δ function
$\bar{\Theta}_E$	mean residence time
$\bar{\Theta}_t$	mean age
σ_E^2	dispersion of distribution of the residence time
ω	revolution frequency

Indices

- e experimental
- c calculated

References

1. Van de Vusse, J. G., *Chem. Eng. Sci.* 17, 507 (1962).
2. Oyama, Y. *et al.*, *Rep. Tokyo Inst. Phys. Chem. Res.* 39, 183 (1963).
3. Cholette, A. and Cloutier, L., *Can. J. Chem. Eng.* 37, 105 (1959).
4. Gianetto, A. and Cazzulo, F., *Chem. Eng. Sci.* 23, 938 (1968).
5. Gibilaro, L. G., *Chem. Eng. Sci.* 26, 299 (1971).
6. Ilavský, J., Brunovská, A., and Košuth, J., *Chem. Zvesti* 29, 620 (1975).
7. Denbigh, K. G., *Chemical Reactor Theory*. Cambridge University Press, London, 1971.
8. Levenspiel, O., *Chemical Reactor Engineering*. J. Wiley & Sons, New York, 1965.
9. Himmelblau, D. M. and Bishoff, K. G., *Process Analysis and Simulation*. J. Wiley & Sons, New York, 1968.
10. Šalát, T. *et al.*, *Malá encyklopédia matematiky*. (Small Encyclopedia of Mathematics.) Obzor, Bratislava, 1978.
11. Hennico, A., Jacques, G., and Vermeulen, T., Univ. of California, Berkeley, Rep. UCRL-10696 (1963).
12. Buffham, B. P. and Gibilaro, L. G., *AIChE J.* 14, 805 (1968).

Translated by R. Domanský